Thermodynamics of a Charged Fermion Layer at High r_s Values

S. Shapira,[1,*] U. Sivan,[1] P. M. Solomon,[2] E. Buchstab,[1] M. Tischler,[2] and G. Ben Yoseph[1]
[1]*Solid State Institute and Physics Department, Technion — Israel Institute of Technology, Haifa 32000, Israel*
[2]*IBM, T. J. Watson Research Center, Yorktown Heights, New York 10598*
(Received 1 August 1995)

The chemical potential μ of a hole layer is mapped as a function of temperature and density p. We present the first investigation of the crossover from the strongly interacting degenerate regime to the classical ideal gas limit. The low temperature inverse compressibility, $\kappa^{-1} \equiv p^2 \partial\mu/\partial p$, is negative and temperature independent. At $T \approx 17$ K temperature dependence commences abruptly: κ^{-1} turns less negative with rising T and eventually reverses sign. An ideal classical gas is attained at temperatures comparable to the interaction energy, more than an order of magnitude larger than the Fermi energy. [S0031-9007(96)01278-1]

PACS numbers: 73.20.Dx, 05.70.Ce, 73.40.Ty

The phase diagram of a two dimensional charged fermion layer is governed [1] by the interplay between the Fermi energy E_F, the Coulomb interaction energy $U \equiv (e^2/4\pi\varepsilon)\sqrt{\pi p}$, and the temperature $k_B T$ (ε is the dielectric constant and p is the carrier density). The corresponding phase space is schematically indicated in Fig. 1 vs two dimensionless parameters, the average interparticle distance measured in Bohr radii, $r_s \equiv U/E_F$, and the classical plasma parameter, $\Gamma \equiv U/k_B T$. Generally, interactions dominate at $r_s, \Gamma \gg 1$, and should ultimately lead to either quantum or classical crystallization at large enough values of these parameters (upper right corner, Fig. 1). As the kinetic energy is increased, the crystal melts into a strongly correlated liquid which turns into an ideal classical (quantum) gas as $k_B T$ (E_F) becomes sufficiently larger than U.

The extreme classical case, $r_s \gg \Gamma$, was extensively studied using 2D electrons on liquid helium [2] in a wide parameter range (marked I in Fig. 1). A classical liquid-solid transition was experimentally observed [3] at $\Gamma = 137, r_s = 3.6 \times 10^3 - 6.1 \times 10^3$. The degenerate regime was primarily investigated utilizing silicon inversion layers [1] and, in recent years, GaAs/AlGaAs heterostructures. The predicted crystallization in the degenerate case has not yet been observed. The very interesting mixed regime, $1 \ll r_s \approx \Gamma$, was barely explored despite the expected intricate crossover [4] between similar classical and quantum mechanical phases.

The portion of phase space accessible with electrons in GaAs/AlGaAs heterostructures, assuming $n \geq 2 \times 10^{10}$ cm^{-2}, is marked II in Fig. 1. The thick line contained within it denotes a recent electron compressibility measurement [5]. Because of the light electronic mass it is limited to $r_s \leq 4$, about a factor of 9 smaller than the theoretically predicted [6] value, $r_s = 37$, for the $\Gamma = \infty$ ($T = 0$) Wigner crystallization. To suppress the kinetic energy we use holes which have a heavier mass than the electrons. The accessible range in phase space for $p \geq 2 \times 10^{10}$ cm^{-2}, assuming $m_h = 0.60 m_0$ [7], is marked III in Fig. 1. To the best of our knowledge, these are the first detailed thermodynamic measurements of degenerate 2D fermions in such a strongly interacting regime.

The thermodynamics of the 2D hole layer is characterized by the chemical potential, $\mu \equiv \partial(p \times F_{2D})/\partial p|_T$, where F_{2D} is the free energy per particle associated with in-plane motion, excluding Hartree terms [see Eq. (2)]. At low densities and temperatures, both μ and its slope, $\partial\mu/\partial p$, are found to be negative [5,8–10]. The reduction in μ as more particles are added to the layer [11] agrees with theoretical calculations [6] of the exchange and correlation contribution to the ground state energy of a 2D quantum liquid, corrected for the finite layer thickness. The chemical potential is found to be temperature independent up to $T \approx 17$ K, where the temperature dependence commences *abruptly* and simultaneously for all hole densities. As the temperature is further raised, $\partial\mu/\partial p$ turns less negative and reverses sign at the low densities first (as expected). This behavior is attributed to a suppression of exchange and other quantum

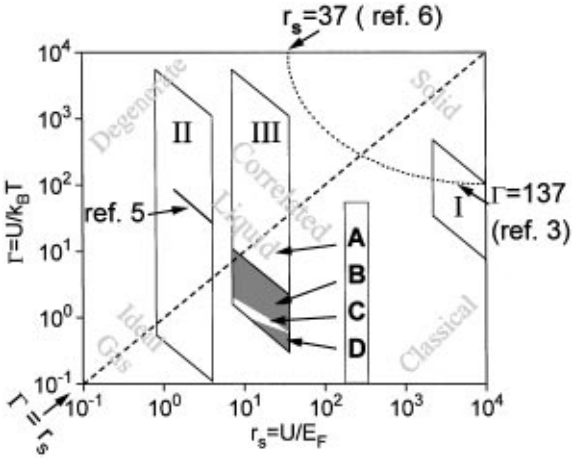

FIG. 1. Schematic phase diagram of 2D charged fermions. I: regime accessible using electrons on bulk helium. II (III): electrons (holes—this experiment) in a GaAs/AlGaAs heterostructure (density $\geq 2 \times 10^{10}$ cm^{-2} and $m_e, m_h = 0.67 m_0, 0.6 m_0$). Four distinct regimes are observed in the experiment labeled A–D (cf. Fig. 4).

correlations with temperature. Remarkably, $\partial\mu/\partial p$ vanishes approximately simultaneously for a broad range of carrier densities indicating an ideal screening at a finite carrier concentration. An ideal classical gas behavior is observed only for $\Gamma \leq 0.65-0.85$, which occurs in our system at temperatures considerably larger than the Fermi temperature (e.g., $T \approx 70$ K compared with $E_F \leq 7$ K for $p \leq 1 \times 10^{11}$ cm^{-2}). At intermediate temperatures, classical correlations apparently dominate $\mu(p,T)$.

The structure [12] was grown by molecular beam epitaxy on an n^+ GaAs substrate. The layers consist of (in growth order) an n^+ buffer layer, 3000 Å intrinsic GaAs, 140 Å (400 Å for a second sample) AlGaAs barrier, 500 Å intrinsic GaAs, 2000 Å $n = 5 \times 10^{16}$ cm^{-3} GaAs, and a 1100 Å $n = 2 \times 10^{18}$ cm^{-3} GaAs cap layer. Upon biasing the top layer negatively enough with respect to the substrate, electron and hole wells are formed on opposite sides of the AlGaAs barrier. Details of the device fabrication and operation are given in Ref. [12]. The samples are processed in a Hall bar shape and may be envisaged as a four plate capacitor (inset of Fig. 2), the two middle plates being the electron and hole layers. The electron and hole concentrations are independently controlled by V_{gn}, $V_{\rm sub}$, and simultaneously varied by V_{pn}. The mobilities and concentrations of both layers are monitored via measurement of the longitudinal and the Hall resistances at a low magnetic field (usually 0.4 T).

The experimental technique [5] consists of a simultaneous measurement of the electron and hole layer concentration as the holes are continuously depleted by $V_{\rm sub}$ at a constant V_{pn} and V_{gn}. Because of the finite screening ($\partial\mu/\partial p \neq 0$) of the hole layer, the electronic concentration n is also modified. The hole chemical potential is then extracted from the variation of n with p. In the special case of two infinitely thin layers (derived in Ref. [5]) the relation assumes a simple form,

$$\mu(p,T) - \mu(0,T) = -\frac{e^2}{\varepsilon}(s + d_n)[n(p) - n(0)]. \tag{1}$$

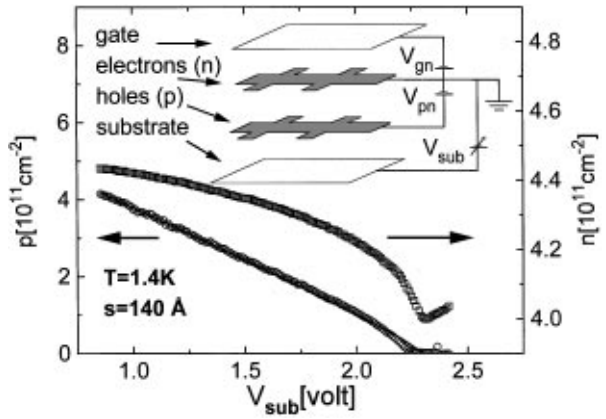

FIG. 2. Hole (circles) and electron (squares) densities vs $V_{\rm sub}$ at a constant V_{pn}, V_{gn}. Solid line: corrected hole concentration (see text). Inset: The system as a four plate capacitor.

Here, s is the AlGaAs barrier thickness, $\varepsilon = 12.5(10.5)\varepsilon_0$ is the GaAs (AlGaAs) dielectric constant, and $d_n = (\varepsilon/e^2)\partial\mu_n/\partial n \ll s$ is the electron screening length which is approximately constant during the measurement. Because the real layer has a finite thickness, additional, small changes in n are induced by Hartree effects. We account for these using the procedure described in the next paragraph. The strength of this method, as demonstrated by Eq. (1) and explained in Ref. [5], is in the fact that n varies mostly due to exchange and correlations which dominate $\mu(p,T)$ in the hole layer. Thus the large Hartree term present in a standard two plate capacitive measurement does not affect the variation of n.

The total free energy of the three plate system consisting of the electron and hole layers and the substrate, coupled to two batteries $V_{pn}, V_{\rm sub}$, is given by

$$F = (F_{\rm 2D} + T_z + E_g)p - epV_{pn} - e(n - p)V_{\rm sub} + U_e + nF_{n\rm 2D}, \tag{2}$$

where E_g is the GaAs band gap, T_z is the hole kinetic energy perpendicular to the plane, U_e is the system's Hartree energy, and $F_{n\rm 2D}$ is the electronic 2D free energy. Using the variational wave functions of Ref. [13] for the holes, U_e, T_z, and hence F are expressed in terms of p, n, and the hole wave-function inverse width b. Minimization of F with respect to these parameters results in three equations, $\delta F/\delta p = \delta F/\delta n = \delta F/\delta b = 0$, that are numerically solved to evaluate $\mu(p,T)$ from the $n(p)$ data. The additional electron gate is neglected in the analysis due to the small variation of the substrate field penetrating *both* layers.

Typical data for p and n vs $V_{\rm sub}$ at $T = 1.4$ K are depicted in Fig. 2. The Hall voltage cannot be used to determine $p < 1 \times 10^{11}$ cm^{-2}. Its magnitude in this range depends on the magnetic field polarity. The hole density (solid line) is then obtained relying on an accurate measurement of n and the fact that the total charge, $e(p - n)$ should vary linearly [5] with $V_{\rm sub}$ for all p, since the substrate is separated from the hole layer by a distance much larger than s. The interesting physics rests with the dependence of n upon $V_{\rm sub}$. Counterintuitively, n decreases as holes are depleted, indicating a *negative* screening or inverse compressibility of the hole layer [cf. Eq. (1)]. Such an effect results from the large exchange and correlation interactions and reflects the large r_s numbers attained. The resulting low temperature chemical potential is negative and considerably larger in absolute value than that of an ideal fermion gas.

Generally, negative compressibility leads to a thermodynamic instability. It is hence emphasized that the chemical potential measured is derived from $F_{\rm 2D}$ which is only a part of the total free energy F of the system [cf. Eq. (2)]. The latter also includes a large positive electrostatic term due to the attraction between the holes and the compensating charge in the adjacent layers. This term stabilizes the system. In other words the chemical

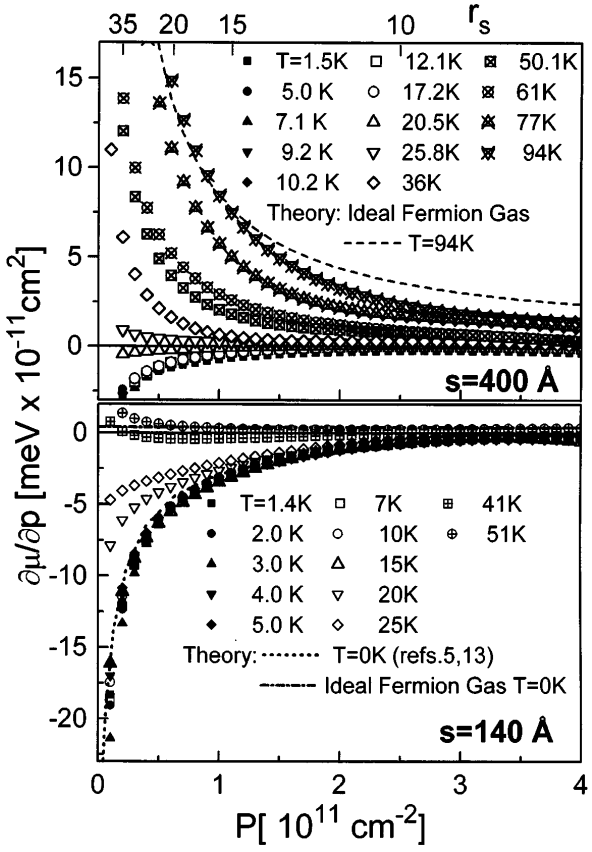

FIG. 3. $\partial\mu/\partial p$ vs p for various temperatures. Top axis: r_s values. Theoretical curves and r_s values assume $m_h = 0.6m_0$.

potential we discuss is measured relative to the subband level in the hole well.

The chemical potential was measured in temperatures up to 51 and 94 K for the $s = 140$ and 400 Å devices, respectively. Maximal temperatures were dictated by barrier leakage. The resulting $\partial\mu(T, p)/\partial p$ are qualitatively similar for the two devices (Fig. 3). The magnitude of the low temperature $\partial\mu/\partial p$ is, however, larger by a factor of 3 in the $s = 140$ Å device than in the $s = 400$ Å one. The dotted curve in the bottom plate of Fig. 3 are the theoretical values for the zero temperature $\partial\mu/\partial p$. They were derived using the numerical calculations of Tanatar and Ceperley [6] taking into account the suppression of exchange and correlation due to the finite layer thickness [14]. It was assumed that exchange and correlation were identically modified by the finite layer thickness. The mass value used, $m_h = 0.60m_0$, leads to a very good agreement with the $s = 140$ Å data, far better than $m_h = 0.38m_0$ (both mass values are based on cyclotron resonance measurements [7] done on a 2D hole layer with similar parameters). However, since the $s = 400$ Å data describe a factor of 3 times similar $\partial\mu/\partial p$, this good agreement is probably fortuitous.

The dependence of $\partial\mu/\partial p$ on the barrier width suggests the importance of interlayer correlation effects [15], which are expected to be enhanced by electron hole attraction [16]. The results were nevertheless independent upon $n(p = 0)$ for $4 \times 10^{11} \geq n \geq 2.8 \times 10^{11}$, $4 \times 10^{11} \geq n \geq 1.3 \times 10^{11}$ cm^{-2} for the $s = 140$ and 400 Å devices, respectively.

The temperature dependence of the data is depicted in Fig. 4 (and 3). We find it can be described by four distinct regimes (marked A–D in Figs. 1 and 4). At temperatures lower than 17 K (regime marked A), the data are practically temperature independent for all hole concentrations for both samples. This temperature independence is consistent with $U/k_B \geq 30$ K for $p \geq 2 \times 10^{10}$ cm^{-2} (where the hole channel becomes insulating). The temperature dependence, however, appears *abruptly* in both samples at $\approx$17 K (vertical dotted line in Fig. 4), simultaneously at all hole densities, possibly suggesting a phase transition. Since such a behavior is unexpected, we have carefully looked for conceivable sources of experimental artifacts including ac and dc leakage, nonlinearities, hole freeze-out, heating of the hole channel, contact resistance, etc., but could not find any in the range of the data reported here. The same abrupt temperature dependence appears also in the hole mobility.

As the temperature is further raised (the intermediate regime marked B is entered), $\partial\mu/\partial p$ gradually turns less negative and reverses sign, first at low densities, at $T \approx 40, 25$ K for the $s = 140, 400$ Å devices, respectively. Despite the fact that the crossover, $\partial\mu/\partial p = 0$, occurs at different temperatures, it is almost density independent in both devices for a broad range of hole concentrations (intersection of solid lines in Fig. 4 and almost flat curves in Fig. 3). The change of $\partial\mu/\partial p$ at intermediate temperatures is roughly linear in T with a slope very similar to an ideal gas (compare to dashed and to dotted lines in Fig. 4). We attribute the reduction in $\partial\mu/\partial p$ to a gradual weakening of the exchange and quantum correlation effects. In particular, the perfect screening ($\partial\mu/\partial p = 0$) at a finite density reflects the compensation of interaction effects by the kinetic energy. Classical correlations, on the other hand, are expected to persist up to $\Gamma \approx 1$. Indeed, in the $s = 400$ Å device, where high temperature data can be obtained, we find an experimental crossover (marked C) to an ideal classical gas, $\partial\mu/\partial p = k_B T/p$, which is attained at $\Gamma = 0.65 - 0.85$ [$T = 70 - 94$ K for $p = (1.2 - 0.4) \times 10^{11}$ cm^{-2}, regime marked D], thus confirming the validity of the experimental method. The temperatures at which an ideal gas is attained correspond to energies an order of magnitude larger than E_F, which demonstrates that the data are dominated by interactions. The physics, in the density ranges accessed in this experiment, is therefore expected to be insensitive to the mass value.

The hole mass, $m_h \sim (0.3 - 0.6)m_0$ is not precisely known. Experimentally, the electronic density determines the electric fields in the hole layer AlGaAs interface and hence the hole well shape. The independence of the data on $n(p = 0)$ demonstrates that even if the effective mass is affected by these changes of the well shape, they are not sufficient to affect the compressibility.

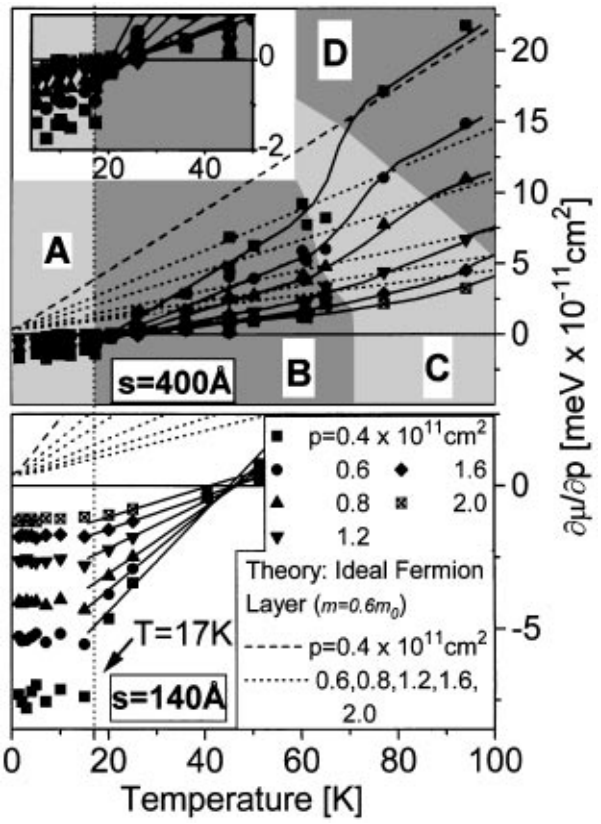

FIG. 4. $\partial\mu/\partial p$ vs T for various hole concentrations. Four distinct regimes are observed: A. Low ($T = 0$) temperature behavior; B. Intermediate regime; C. Crossover regime; D. Classical ideal gas. The straight lines in regime B denote linear regression. Inset: expanded low temperature data for the $s = 400$ Å device. The bottom temperature axis refers to both plates and the inset.

A sharp change in the hole dispersion may be more important. Detailed Shubnikov–de Haas and low field magnetoresistance measurements indicate, however, a simple band structure up to $p_c = 2.5 \times 10^{11}$ cm^{-2}, above which an additional band appears. For $p > p_c$ our SdH data reproduce previously reported data [7] on a similar 2D hole layer.

In summary, the thermodynamics of a two dimensional hole layer at unprecedented large r_s numbers was characterized by chemical potential measurements. Four distinct regimes have been mapped in the density-temperature plane (Figs. 1 and 4). At low temperatures, μ and $\partial\mu/\partial p$ are negative and qualitatively agree with theory [6,14]. They are temperature independent up to $T \approx 17$ K where the temperature dependence appears abruptly for all hole densities. The dependence of $\partial\mu/\partial p$ on temperature is at first very similar to that of an ideal classical gas, $\partial\mu/\partial p = k_B T/p$, shifted down by a constant value. As the temperature is further increased, $\partial\mu/\partial p$ reverses sign almost simultaneously at all hole densities, indicating a metallic screening at finite densities and temperatures. At higher temperatures a crossover is observed to an ideal classical gas which is attained at temperatures higher than the interaction energy ($\Gamma \leq 0.65 - 0.85$) and almost an order of magnitude higher than the degeneracy temperature.

The agreement of the low (up to a constant) and high temperature compressibility with theory prove the validity of the experimental method. We hope that the understanding of the intermediate temperature data will pose a challenge to both theorists and experimentalists.

We acknowledge useful discussions with L. Pitaevskii, A Macdonald, J. Eisenstein, and M. Kastner. The work was supported by the Binational Science Foundation (BSF) and by a Technion grant for the promotion of research.

*Present address: Cavendish Laboratory, Madingley Road, Cambridge CB3 0HE, United Kingdom.

[1] A general review of the field with an emphasis on works in silicon MOSFETs is found in T. Ando, A. B. Fowler, and F. Stern, Rev. Mod. Phys. **54**, 437 (1982).
[2] P. Liederer, J. Low. Temp. Phys. **87**, 247 (1992), and references therein.
[3] C. C. Grimes and G. Adams, Phys. Rev. Lett. **42**, 795 (1979).
[4] M. Imada and M. Takahashi, J. Phys. Soc. Jpn. **53**, 3770 (1984); F. M. Peeters and P. M. Platzman, Phys. Rev. Lett. **50**, 2021 (1983).
[5] J. Eisenstein, L. Pfeiffer, and K. West, Phys. Rev. Lett. **68**, 674 (1992); J. P. Eisenstein, L. N. Pfeiffer, and K. W. West, Phys. Rev. B **50**, 1760 (1994).
[6] B. Tanatar and D. M. Ceperley, Phys. Rev. B **39**, 5005 (1989).
[7] H. L. Stormer, Z. Schlesinger, A. Chang, D. C. Tsui, A. C. Gossard, and W. Wigmann, Phys. Rev. Lett. **51**, 126 (1983).
[8] S. V. Kravchenko, V. M. Pudalov, and S. G. Semenchinskii, Phys. Lett. A **141**, 71 (1989).
[9] P. M. Solomon, U. Sivan, and H. Shtrikman, in *Proceedings of the 10th International Conference on the Electronic Properties of the Two Dimensional Systems, Newport, RI 1993*.
[10] B. E. Kane, J. P. Eisenstein, W. Wegscheider, L. N. Pfeiffer, and K. W. West, Appl. Phys. Lett. **65**, 3266 (1994).
[11] In the 3D case see, e.g., G. D. Mahan, *Many Particle Physics* (Plenum Press, New York, 1993), pp. 462–466.
[12] U. Sivan, P. M. Solomon, and H. Shtrikman, Phys. Rev. Lett. **68** 1196 (1992).
[13] F. F. Fang and W. E. Howard, Phys. Rev. Lett. **16**, 797 (1966).
[14] F. Stern, J. Appl. Phys. Suppl. 2 Pt. **2**, 323 (1974).
[15] L. Zheng and A. H. Macdonald, Phys. Rev. B **49**, 5522 (1994).
[16] L. Swierkowski, J. Szymanski, and Z. W. Gortel, Phys. Rev. Lett. **74**, 3245 (1995).